Characterization of Plastically Compressed Collagen Hydrogels With and Without Silver Nanoparticles for Tissue Repair

Luka Vukovic
8593417

BIM4009: Research Project - Biomedical Science

Presented to:
Dr. Emilio Alarcon

Research Advisor:
Dr. Christopher McTiernan

uOttawa

Department of Chemistry and Biomolecular Sciences
April 17th, 2020

1. Abstract

Diabetic foot ulcers (DFUs) are chronic wounds which extend through the dermis and are characterized by neuropathy, ischemia, and infection. With an estimated 5-year mortality rate of 42% (Everett and Mathioudakis, 2018), it is apparent that current treatments for DFUs need further improvement. A potential solution for longterm wound closure is the use of collagen hydrogels as scaffolds for skin regeneration. While the biocompatibility, antigenicity, and similarity to the fibroblast extracellular matrix make collagen-based biomaterials an ideal candidate for improving the skin's regenerative capacity, they are typically susceptible to degradation by bacterial collagenases and carry no antiseptic properties. Herein, we have generated soft hydrogels using medical grade Type I porcine collagen (Theracol) and attempted to modify their physical properties and resistance toward degradation through plastic compression. Furthermore, we have begun to explore whether functionalization with silver nanoparticles (AgNPs) could provide a means for antiseptic action without fibroblast cytotoxicity. To assess degradability and cytotoxicity; collagenase, cell proliferation, and live/dead assays were performed along with a battery of other physical characterizations. While plastic compression alone did not significantly improve resistance towards collagenase degradation, functionalization of the hydrogels with AgNPs decreased the rate of collagenase degradation by a factor of ≈ 2 for non-compressed hydrogels and ≈ 10 for compressed hydrogels. However, functionalization of the hydrogels with AgNPs appears to decrease their biocompatibility, with lower proliferation of human dermal fibroblasts observed on the AgNP functionalized gels, which can be attributed to a lower number of viable cells on these materials. Our work shows that plastic compression of Theracol hydrogels and the introduction of AgNPs can enhance collagenase resistance; however further optimization

of the functionalization process as well as improvements to post-functionalization treatment may be required to improve biocompatibility.

2. Acknowledgments

With utmost appreciation and gratitude, I would like to thank my principal investigator, Dr. Emilio Alarcon, and my post-doctoral supervisor, Dr. Christopher McTiernan for their investment of time and attention into supporting my work throughout this project. I would also like to thank the rest of the BioEngineering and Therapeutic Solutions (BEaTS) Division of Cardiac Surgery lab, without whom such work would not have been made possible.

Table of Contents

3. Statement of Contributions

The creation of figures and revision of the following thesis was done with the guidance of Dr. Christopher McTiernan.

4. Introduction

Diabetes mellitus is a condition of chronic hyperglycemia that can lead to neuropathy, peripheral artery disease, and diabetic foot ulcers (Everett and Mathioudakis, 2018). An increased risk for peripheral artery disease can contribute to ischemia in the extremities. Without sufficient perfusion of blood to the hands and feet, susceptibility to infection increases while the regenerative potential of tissue decreases. In combination with diabetic neuropathy, normally painful injuries to the extremities, such as punctures and cuts, may easily go unnoticed due to a lack of innervation. If wounds go unobserved for too long and healing at the site does not occur to a reasonable degree, the wound can ultimately develop into a diabetic foot ulcer (DFU). DFUs can be defined as poorly healing full thickness wounds that extend through the dermis, occurring below the ankle in individuals with diabetes or other risk factors that promote ischemia, neuropathy, or infection. Prevalence of DFUs in North America is 13.0% (Zhang *et al.*, 2016) and the estimated 5-year mortality rate is a stark 42% (Everett and Mathioudakis, 2018). Being the major cause of amputation in diabetics, DFUs additionally lay a substantial burden on the healthcare system accounting for 33% of all costs of diabetic care (Driver *et al.*, 2010). This is in part due to the chronic nature of DFUs in combination with cost-intensive treatment procedures. Reducing healing times of DFUs can thus alleviate some of this burden while maximizing a patient's longterm prognosis.

Treatments for DFUs include rigorous antibiotic regiments, wound debridement procedures, wound off-loading to reduce pressure on site, and dressings that offer a moist healing environments. Still however, current treatments that attempt to control infection and ensure wound closure do not securely improve a patient's long-term quality of life. Prolonged use of antibiotics risks the development of antibiotic resistant infections, and no current wound dressing can

consistently achieve all three requirements of symptom alleviation, wound protection, and healing (Hilton *et al.*, 2004).

A potential solution to both ineffective wound dressings and septic control are hydrogel biomaterials. Hydrogels are 3D networks of hydrophilic polymer chains that absorb large quantities of water, essential for maintaining moisture at the site of infection (Chai *et al.*, 2017). Thus, collagen hydrogels are 3D networks of collagen polymers (Figure 1). To provide broad antiseptic properties, they can be functionalized with metal nanoparticles (Alarcon *et al.*, 2015). Clinical work on collagen hydrogels suggest they can outperform basic wound dressings, and despite products such as Woun'Dres®, HELIX3®, and Dermagraft® already being commercially available, limited study designs and research biases leave their status somewhat inconclusive (Dumville *et al.*, 2013; Holmes *et al.*, 2013). Thus, uncertainty in effectiveness hints that collagen hydrogels can still be improved.

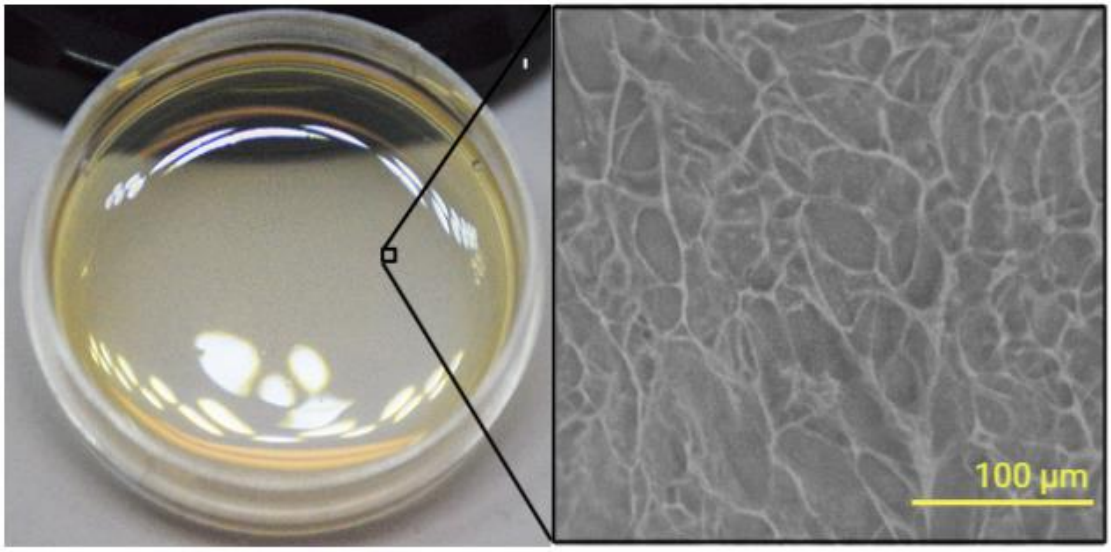

Figure 1. Collagen hydrogel biomaterial (left) prepared from medical grade Type I porcine collagen and cryogenic scanning electron microscopy image (right) of the 3D hydrophilic collagen polymer network. Preparation detailed in 5.1.

What renders collagen hydrogels an ideal candidate for application in DFUs are the following factors: collagen's biocompatibility, antigenicity, and similarity to the fibroblast extracellular matrix that emulates physiological conditions better than other wound dressings. Primary issues underlying collagen hydrogels is that they have weak mechanical properties (Chai *et al.*, 2017), are susceptible to degradation by bacterial collagenases, and carry no antiseptic properties without further functionalization. Antiseptic properties can be improved with the functionalization of antibiotics, antimicrobial peptides, synthetic drugs, as well as metal nanoparticles (NPs) (Li *et al.*, 2018). The mechanism of NP antiseptic activity is particularly unique and may serve as an attractive alternative to antibiotics especially with the rise of antibiotic resistance. NPs are thought to form complexes with critical proteins in the respiratory chain, catalyze formation of reactive oxygen species to induce DNA damage, and to also bind directly to DNA inhibiting cell replication (Slavin *et al.*, 2017). However, powerful and broad antimicrobial mechanisms of action also increase the risk for cytotoxicity in humans. Thus, NP design, characterization and assessment of biocompatibility is a thorough process. If done correctly, prior literature describes that metal NPs can possess anti-inflammatory properties, anti-viral properties, and most importantly broad antiseptic properties that reduce the risk for antibiotic resistance (Singh *et al.*, 2018; Galdiero *et al.*, 2011; Teow *et al.*, 2018).

Metal NPs are defined as pure metal bodies ranging from 1 to 100nm, substantially smaller than visible wavelengths of light (400-700nm). In neutral (reduced) states, pure metal supports collective oscillation of electrons which are termed as plasmons (Figure 2). When the frequency of incoming electromagnetic radiation matches the frequency of electron oscillation, a resonant state is established that causes extremely high localized heating at the surface of NPs. This effect is termed surface plasmon resonance (SPR). Because SPR (absorption of electromagnetic waves)

occurs at wavelengths within the visible spectrum of silver (Ag) and gold (Au) metal NPs, we can perceive colouration in colloidal NP solutions for these metals. Many factors can affect the colouration, such as changes in particle concentration, size, 3D shape, and surface ligands. Colouration is particularly important to note when functionalizing hydrogels with NPs since it can hint at what type of NP resides on the material. SPR may also support mechanisms for antiseptic activity via localized heating and protein denaturation. This paragraph explains theory sought from "Silver nanoparticle applications: in the fabrication and design of medical and biosensing devices" (Alarcon *et al.*, 2015).

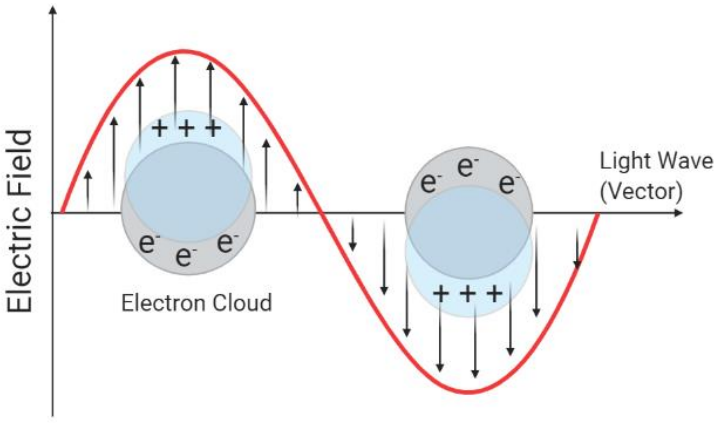

Figure 2. Schematic representation of metal nanoparticle (spherical) plasmon excitation upon exposure to a wavelength of electromagnetic radiation that induces plasmon resonance. This figure was adapted and reconstructed from theory in Kevin Stamplesoskie's, "Silver Nanoparticles: From Bulk Material to Colloidal Nanoparticles" (Alarcon *et al.*, 2015).

Noble metals such as neutral copper, silver, and gold are non-toxic to humans so are often the choice for nanoparticle development. However, it is the oxidation product of metal NPs that can render them toxic, threatening NP biocompatibility (Asharani *et al.*, 2009). For this reason, it is of utmost importance to maintain NP colloidal stability to prevent NP aggregation and oxidation throughout the DFU healing process. Zeta potential is a measure of particle surface charge, so the

stronger the surface charge (zeta potential), the less likely colloidal particles of the same charge are to aggregate and oxidize. Reduced metals will have a neutral charge until their surface begins to oxidize to create a cationic coating. At this point, negatively charged capping agents like citrate and other thiol containing peptides can be used to stabilize surfaces via electrostatic interactions (Poblete *et al.*, 2018). Copper NPs for example oxidize easily within minutes, particularly if exposed to air, and will release cytotoxic Cu^{2+} into the periphery. Its lack of stability has limited its application in biomaterials (Cushing *et al.*, 2004). Gold by contrast is the most stable noble metal, however, silver was chosen for this project since prior pre-clinical work has implemented biocompatible collagen protected silver NPs (Alarcon *et al.*, 2015) and silver's ability to penetrate human skin is much lower than that of gold, reducing the risk for systemic exposure (Wang *et al.*, 2016).

We present two hypothetical assumptions. Firstly, that plastic compression of collagen hydrogels can increase hydrogel stiffness by increasing collagen network density (reducing the average pore size), and as a result aid in improving gel mechanical properties. Second, that functionalization of compressed hydrogels with citrate/collagen protected AgNPs will continue to provide antibacterial properties without human cytotoxicity. Thus, the purpose of this project is to characterize new hydrogel formulations that yield improved properties of degradability without additional cytotoxicity from functionalization with antiseptic AgNPs.

Herein, we have generated soft hydrogels using medical grade Type I porcine collagen (Theracol) (Figure 1) and developed an *in situ* protocol for photochemically functionalizing AgNPs so that they are supported by collagen. There are multiple preparation methods that can be used to integrate AgNPs. These are summarized in Figure 3.

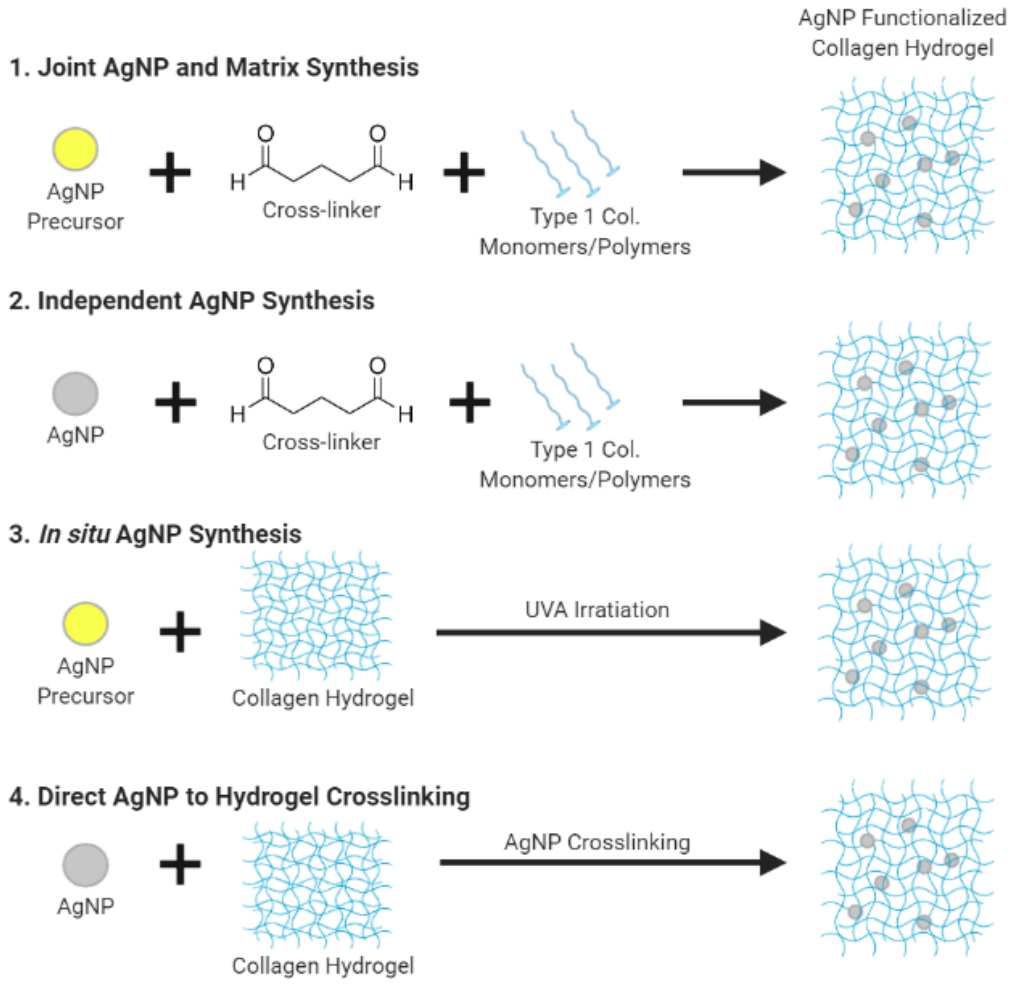

Figure 3. Different methods for functionalization of collagen hydrogels with AgNPs. This figure was adapted from a similar summary produced by Hui-Li *et al.* (2019).

We assessed hydrogel degradability via a collagenase assay, and upon no significant improvements from plastic compression proceeded to characterize hydrogel stiffness with rheological measures and average pore size with cryogenic scanning electron microscopy (Cryo-SEM). Cell viability on the hydrogels was assessed via cell proliferation and live/dead assays. Throughout this project, non-compressed collagen hydrogels (H) were used as controls for plastically compressed hydrogels (CH), while non-functionalized hydrogels acted as controls for

AgNP functionalized hydrogels (Figure 4). To better illustrate how hydrogels appear after plastic compression, we've included Figure 5 in the methods section.

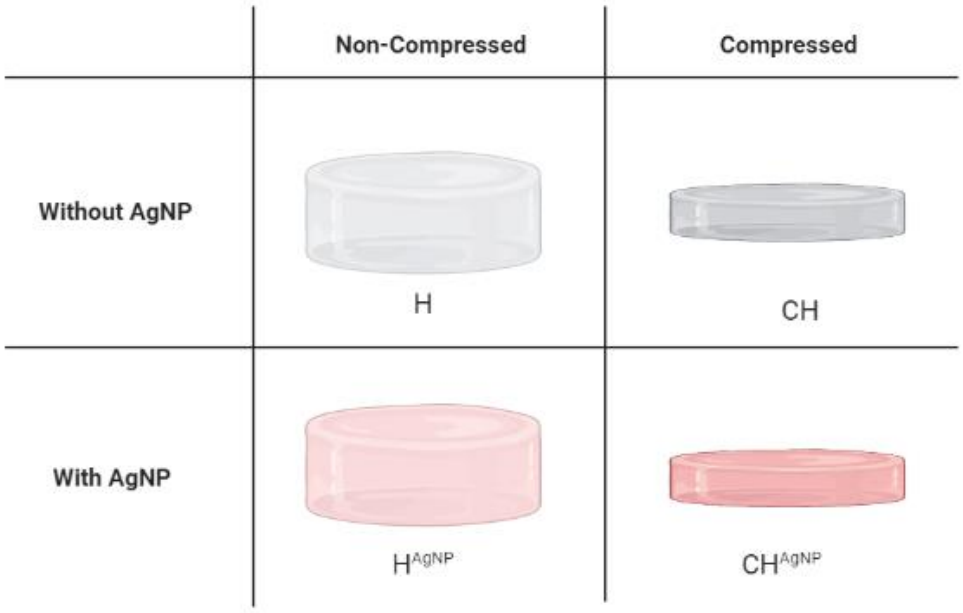

Figure 4. The four categories of developed experimental collagen hydrogels. Hydrogel (H), Compressed Hydrogel (CH), Hydrogel with AgNP (H^{AgNP}), Compressed Hydrogel with AgNP (CH^{AgNP})

Results suggest that our method of plastic compression did not modify the parameters of interest (stiffness and pore size) and did not significantly affect the collagenase degradation rate. As such, an alternative method for compression may yield more confidence into understanding the true physical and biological implications of plastic compression. Our results also suggest that the AgNPs generated *in situ* were not stable and brought on cytotoxic effects. Many factors can affect AgNP stability so parameters for AgNP functionalization may need to be adjusted. The stability of AgNPs should be assessed using different functionalization techniques and can be assessed by measuring the surface plasmon resonance before and after addition of NaCl solution which favours Ag^0 to Ag^+ conversion. Salt induced destabilization of AgNP is probably due to chloride ions acting as Ag^+ sinks, complexing to form insoluble silver chloride (nanoComposix©, 2020). This

would effectively strip Ag^{+} from solution and surfaces of poorly protected AgNPs, shifting the equilibrium between Ag^{0} and Ag^{+} to render silver oxidation more enthalpically favourable. Ultimately, the rate and extent of AgNP oxidation at different salt concentrations would help in quantifying AgNP stability after its *is situ* hydrogel synthesis.

5. Methods

Chemicals

1% w/v Theracol is a medical grade porcine type I collagen solution that was used as received (TheraCol, Sewon Cellontech, Seoul, South Korea). Collagen medium (10x) was prepared from 9mL of 10x DMEM, 9mL of 10x HEPES, 10mL of FBS, and 0.1mL of gentamycin. DMEM is Dulbecco's modified eagle medium (pH ≈7.2). HEPES is from Waterman-Storer and Waterman-Storer, 2001. FBS is fetal bovine serum. PBS is phosphate buffer saline (pH 7.2) prepared from tablets obtained from Sigma-Aldrich. NaOH is sodium hydroxide. AgNPs is silver nanoparticles. Silver nitrate ($AgNO_3$) and citrate ($Na_3C_6H_5O_7$) were purchased from Sigma-Aldrich. I-2959 is Irgacure-2959 (2-Hydroxy-1-[4-(2-hydroxyethoxy) phenyl]-2-methyl-1-propanone) purchased from Sigma-Aldrich. Tris base is tris(hydroxymethyl)aminomethane buffer (Tris 0.1 M at pH 9.0). Tris-HCl buffer is 12.11g of Tris base and 0.55 calcium chloride added to 1000mL of water whose pH was adjusted to 7.4 using HCl. Type I Collagenase was obtained *Clostridium histolyticum* (250 U per mg solid, Sigma). Glutaraldehyde was sourced from Sigma-Aldrich.

5.1 Collagen Hydrogel preparation

Collagen hydrogels were prepared in a sterile biosafety cabinets using a cross-linking agent, glutaraldehyde, at pH 7.2-7.4, followed by neutralization with glycine solution to end the reaction after 12 minutes. The reaction took place on ice, without any light, and the reaction medium contained Theracol solution, collagen medium, PBS, and NaOH to adjust pH since collagen medium is slightly acidic. Hydrogels were then left at 4°C for 30 minutes, followed by a 1 hour gelation period at 37°C. To prevent dehydration after preparation, PBS or Milli-Q water was added to the plate which was then stored at 4°C for future use.

5.2 Plastic compression

A 3D printed plastic compression device (Figure 5) was developed in 3D CAD software and printed with an Ultimaker S5 using PLA filament. It contains holes (2mm diameter) to let water escape when applying pressure to hydrogels. Pressure was applied until water was seen exiting >75% of holes on the device and left to sit for 3min under that constant pressure. Expelled fluid was carefully blotted off the edges of the hydrogel with Kimtech Kimwipes.

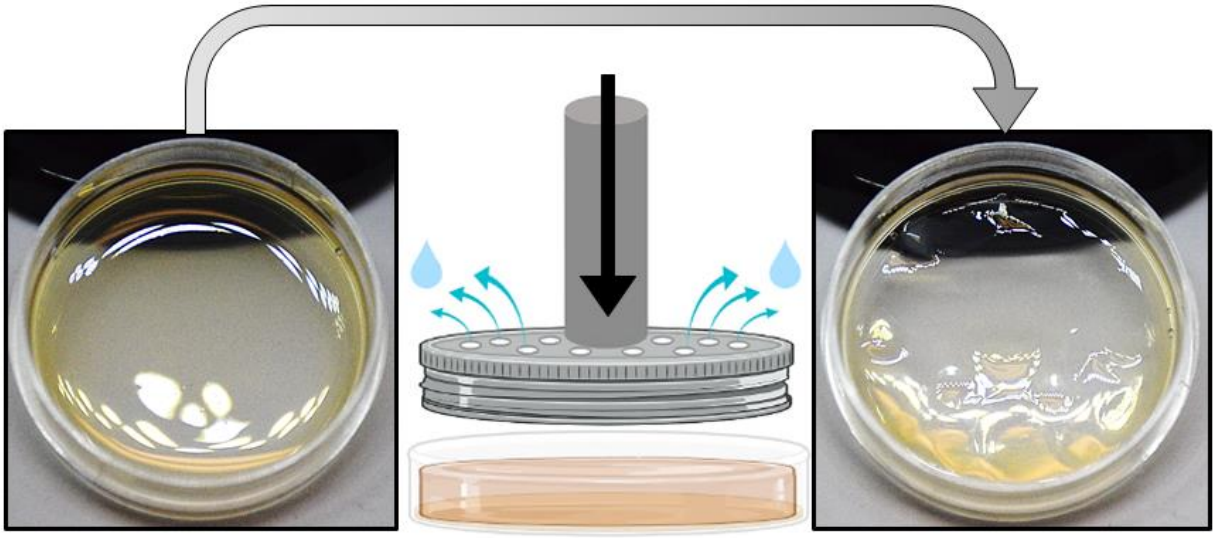

Figure 5. Illustration of plastic compression procedure using the 3D printed plastic compression device. Collagen hydrogel before (left) and after (right) plastic compression. Pores passing through the device allow water to escape as the hydrogel is compressed for three minutes.

5.3 In situ functionalization of Collagen with AgNPs

Collagen hydrogels were initially prepared as in section 5.1 followed by an overnight wash with Milli-Q water to remove PBS that could destabilize AgNPs. The following day, hydrogels were submerged in an AgNP reagent mixture of $AgNO_3$ [0.36 mM], I-2959 [0.36 mM], and citrate [1.79 mM]. After submersion, supernatant was replaced with Nitrogen purged Milli-Q water and

irradiated in a UVA Luzchem CCP-4 V photoreactor fitted with 12 UVA lamps at 25.0 ± 0.5°C for 10 minutes, resulting in AgNP functionalized collagen hydrogels.

5.4 Preparation of Citrate Protected Colloidal Silver Nanoparticles (AgNP)

A solution of 0.2 mM $AgNO_3$, 0.2 mM I-2959, and 1.0 mM citrate was purged of oxygen with nitrogen gas for 30 minutes then irradiated in a UVA Luzchem CCP-4 V photoreactor fitted with 12 UVA lamps at 25.0 ± 0.5°C for 10 minutes.

5.5 Collagenase Assay

Collagenase solution: Collagenase solution was prepared the same day as the experiment. 200mL of collagenase solution was prepared at 5units/mL by adding 4mg (1000 units) of Type I collagenase to 200mL of Tris-HCl buffer.

Collagen hydrogels were made one day prior to analysis. Hydrogels were then washed 3 times for 15 minutes and let to soak in the 3rd wash overnight. The following day, hydrogels were washed with 1xPBS or Milli-Q® in the case of AgNP functionalized hydrogels to avoid AgNP oxidation. Hydrogels were then cut into 10-20mm pieces and incubated in Tris-HCl at 37°C for 1 hour prior to the assay. Hydrogels were submerged in 1.0 – 1.5mL of 5U type I collagenase solution at 37°C. Hydrogel weights were measured at the start (W_0) and at different time intervals (W_t{W_1, W_2, W_3, W_4, W_{24}}). Kimwipes were used to remove excess water by blotting around the hydrogels. Every measurement was followed by the re-addition of 1.0 – 1.5mL of fresh 5U collagenase solution. Calculations were as follows:

The % weight remaining at time *t* :

$$\%wt_t = \frac{W_t}{W_0} \times 100$$

Average 24 hour degradation rate (% weight loss/hour) where $\%wt_0 = 100\%$:

$$\frac{\%wt\ loss}{hour} = \frac{100\% - \%wt_{24}}{24} \times 100$$

The half life equation was rearranged (see all steps in Appendix) where $\boldsymbol{t_{\frac{1}{2}}}$ is the half-life, $\boldsymbol{t}$ is the elapsed time, $\boldsymbol{N_0}$ is the quantity in the beginning (100%), and $\boldsymbol{N_t}$ is the quantity at time *t* ($\%wt_t$):

$$N_t = N_0\ 0.5^{\frac{t}{t_{\frac{1}{2}}}} \quad \text{to} \quad (\%wt_t) = (100\%)\ 0.5^{\frac{t}{t_{\frac{1}{2}}}} \quad \text{to} \quad t_{\frac{1}{2}} = \frac{t \times (-ln2)}{ln\left(\frac{\%wt_t}{100\%}\right)}$$

$t_{1/2}$ was calculated based on $\%wt_4$ (*t* = 4 hours), with the exception of CH^{AgNP} hydrogels, whose half life is based on $\%wt_{24}$ (*t = 24*).

5.6 Water content

The weight of hydrogels submerged in PBS (or Milli-Q water if hydrogels contained AgNP) was measured as the fully hydrated weight (W_0). Hydrogels were desiccated in a vacuum at room temperature until a consistent weight was achieved (W_{dry}) to indicate full dehydration. Solid mass content (SMC) was then calculated using the equation below.

$$SMC = \frac{W_{dry}}{W_0} \times 100$$

5.7 Swelling

Collagen hydrogels were submerged in PBS (gels without AgNP) or Milli-Q water (gels with AgNP) over 7 - 9 days. The gels were weighed after 1, 2, 3, and 7 or 9 days. Excess fluid surrounding gels was removed using Kimwipes prior to weighing.

5.8 Rheology

Approximately 1mL hydrated hydrogel samples approximately 3cm across were subjected to a shear rate of $5s^{-1}$ at a frequency of 1Hz for 600s under a C25-2 spindle on a Brookfield R/S plus rheometer (Brookfield) equipped with Series IX/S software. The C50-2 spindle was used. A gap of 4 μm was set according to the spindle specifications, and the temperature was maintained at 37°C. The Rheo3000 v1.2 software was used to monitor the rheological properties in terms of viscosity (Pa·s).

5.9 Cryo-SEM

Average pore size was obtained via ImageJ software analysis on low temperature scanning electron microscopy (Cryo-SEM) in a Tescan (model: Vega II – XMU) with cold stage sample holder at −50 °C. Cryo-SEM image scales were calibrated on ImageJ, followed by image contrast equalizing and normalizing. All shades of gray in the images were binarized to either black or white using Auto Local Thresholding (Local radius = 20 – 30 μm). Noise was processed to despeckle and remove white or black pixel outliers, giving a cleaner image of hydrogel pores. The analyze particle size was used to measure the area in every pore represented as a white object (area search range: 40 μm^2 – 30’000 μm^2).

5.10 Live/Dead Cell Viability Assay

A cell viability assay on immortalized human fibroblasts was performed 5 days after initial seeding. Cell were seeded in 20 wells at 2500 cells/well (0.75 cm^2). Culture media (DMEM containing 10% fetal calf serum) was renewed every 2 – 3 days. A live/dead cell staining kit (Invitrogen, Burlington, Canada) containing Calcein-AM (green) and ethidium homodimer-1 (red) were used to stain and identify viable and non-viable cells, respectively. Three multichannel images (green field and red field) were taken of each well using a 20x objective on an Olympus IX80 laser scanning confocal microscope operated by FV1000 software v1.4a. Green and red cells were counted for every image and averaged across an experimental group. Green cells were considered viable ("live"), cells containing both green and red were considered apoptotic ("dying"), and red cells were considered dead.

5.11 Proliferation

Green fluorescence protein (GFP) transfected immortalized human fibroblasts cells were seeded in 20 wells at 2500 cells/well (0.75 cm^2). Culture media (DMEM containing 10% fetal calf serum) was renewed every 2 – 3 days. Two to four multichannel images (bright field and fluorescent field) were taken of each well daily for 7 days after initial seeding using a JuLI™ Br Live Cell Analyzer. To avoid imaging cells proliferating below the hydrogel, the edge of the hydrogel's was used to correctly focus onto only the gel's surface. Quantification of cell numbers was carried out using Image-J software.

5.12 Statistical Tests

For all results that involved comparisons between two sample means, t-Tests assuming unequal variances were performed with a significance cut-off point of $p = 0.05$. For pore size distribution analysis (Figure 16) a non-parametric Kolmogorov-Smirnov Test was performed to assess if differences in pore size distribution were significant.

6. Results

6.1 Effects of Compression and AgNP Functionalization on Hydrogel Degradability

AgNP functionalized and compressed hydrogels (CH^{AgNP}) displayed the greatest decrease (improvement) in 24 hour average degradation rate. It had an hourly loss rate that was 33% lower than other experimental groups ($p < 0.001$). Compression alone (CH) did not improve degradability at any point. AgNP functionalization alone (H^{AgNP}) showed some initial improvements in loss rate during the first 4 hours but not over 24 hours. CH^{AgNP} gels had an estimated half life of ≈ 18 hours, H^{AgNP} gels had an estimated half life of ≈ 7 – 9 hours, and non-functionalized gels had a half life at around ≈ 2 hours. Although, H^{AgNP} gels reached the same point as non-functionalized gels by 24 hours.

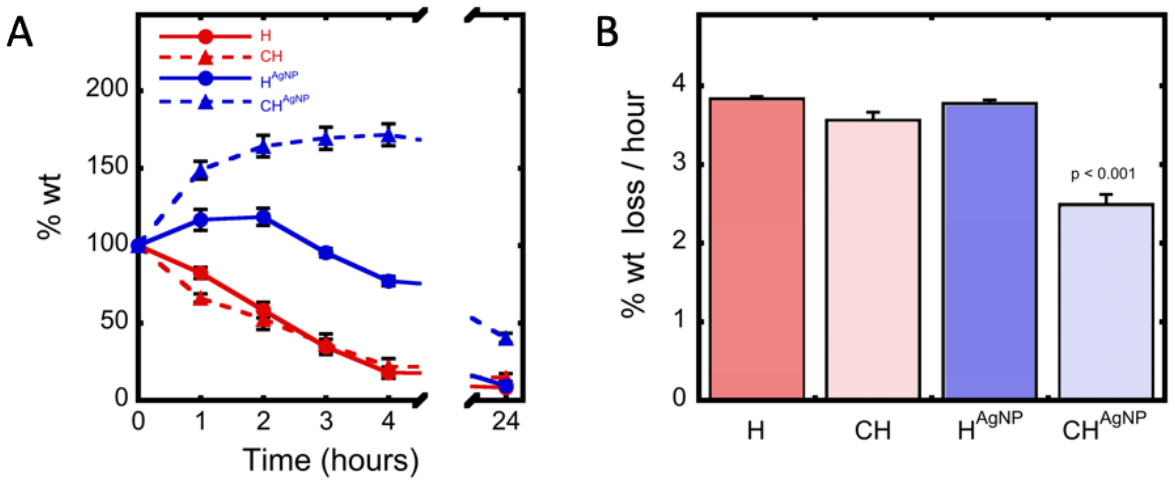

Figure 6. Collagenase assay illustrating hydrogel weight loss (degradation) as a function of time. (A) Percent weight of hydrogels remaining as measured over 24 hour period while submerged in 1mL of 5U type I collagenase solution. Collagen Hydrogels (H) and Compressed Collagen Hydrogels (CH) had a sample size of n=9 whereas hydrogels functionalized with AgNP (H^{AgNP}, CH^{AgNP}) had a sample sizes of n=6. Error bars represent the standard error. (B) The 24-hour average degradation rate of compressed and AgNP functionalized collagen hydrogels (CH^{AgNP}) was 33% lower ($p<0.001$) compared to other hydrogels. The difference between initial weight (100%) and final % wt was divided by 24 hours to yield an average hourly degradation rate. Sample sizes are the same as in A and error bars represent the standard error. Significance was assessed by comparing CH^{AgNP} to each other hydrogel via a two-sample t-Test assuming unequal variances.

6.2 Collagen Hydrogel Functionalization with AgNPs

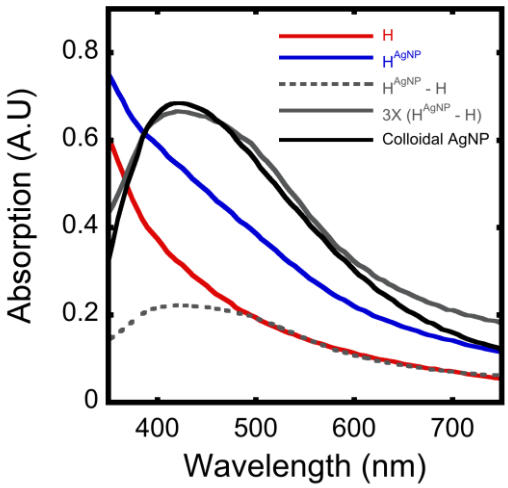

Figure 7. UV-Vis absorption spectra of unmodified and AgNP functionalized hydrogels. Absorption spectrum of AgNP functionalized hydrogels display a shoulder around 400 nm, characteristic of AgNP. UV-Vis absorption spectrum of colloidal citrate protected AgNP resembles the difference spectrum (3X (H^{AgNP} – H)) produced from the difference between hydrogels before (H) and after (H^{AgNP}) UVA irradiation. The difference spectrum was amplified 3x and overlaid on the spectrum of colloidal citrate protected AgNPs. Prior to UV-Vis measurements, hydrogels were washed to remove any weakly bound AgNPs. The process of hydrogel functionalization is detailed in Methods section 5.3. Spectra correspond to the average of n=4 samples. Water was used as a blank in all measurements.

6.3 Physical Characterization of Compressed and AgNP Functionalized Collagen Hydrogels

The method of hydrogel compression (5.2) produced compressed gels with a SMC that was almost double (factor of 1.9) that of non-compressed gels ($p < 0.001$) (Figure 8). This reflects a total compressed weight that is roughly half the total weight of non-compressed gels. For example: 2.5% of 1g is 5% of 0.5g) indicating a 50% decrease in water content by mass. Compression was confirmed to be plastic as no gel decompressed to its original weight during a 7 – 9 day swelling period ($p < 0.001$) (Figure 9).

In Figure 10, non-compressed gels that were functionalized with AgNPs had substantially lower viscosity than other types ($p < 0.05$). Compression did not have an effect on viscosity in AgNP free hydrogels ($p > 0.5$) but seems to have doubled the viscosity of AgNP containing gels.

This doubling could not however be considered significant due to the limited sample size of AgNP functionalized hydrogels (n = 2).

Frequency distribution of collagen pore sizes as a diameter based on representative Cryo-SEM images revealed that non-compressed gels had a mean pore size roughly 9 μm smaller than compressed gels (Figure 11). Additionally, a Kolmogorov-Smirnov cumulative distribution test between the collagen pore size areas (μm^2) of non-compressed and compressed gels is shown in Figure 16 (Appendix). Compressed gels have pore sizes that are on average larger and more dispersed (mean = 1196; median = 291; standard deviation = 2528) than pores of non-compressed hydrogels (mean = 413; median = 160; standard deviation = 814) ($p < 0.0005$).

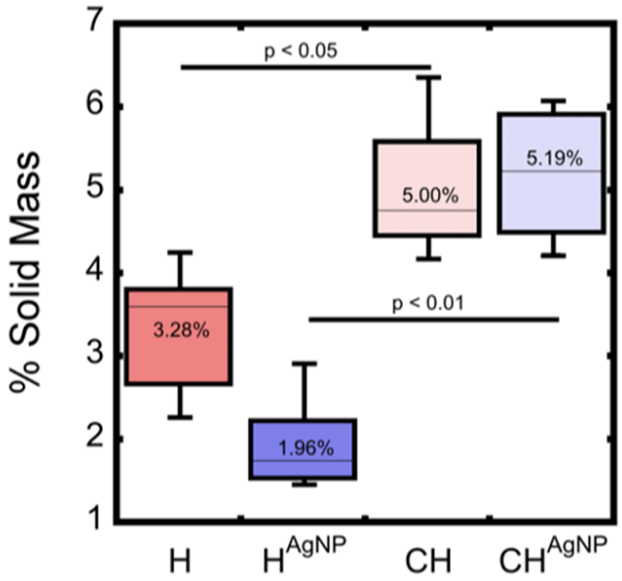

Figure 8. Solid mass content (SMC) of unmodified collagen hydrogels (H), compressed collagen hydrogels (CH), and collagen hydrogels with AgNPs (H^{AgNP}, CH^{AgNP}). Compression of collagen hydrogels, with and without AgNPs induced significant increases in SMC ($p < 0.03$, $p < 0.002$ respectively) by an average factor of roughly 1.9 times ($p < 0.0001$; not in figure). Mean SMC was 2.67% for non-compressed gels and 5.10% with compression when including AgNP functionalized hydrogels. The method of compression and AgNP functionalization is detailed in 5.2 and 5.3 respectively. Sample sizes: H(n=7), CH (n=4), H^{AgNP}(n=6), and CH^{AgNP}(n=4). Group sample means are labeled in each boxplot.

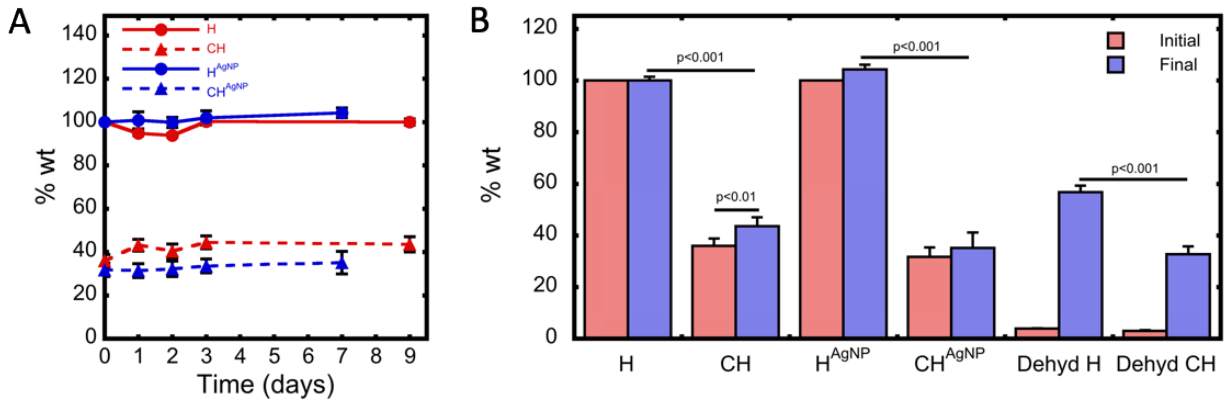

Figure 9. Swelling capacity of unmodified collagen hydrogels (H), compressed collagen hydrogels (CH), collagen hydrogels with AgNPs (H^{AgNP}, CH^{AgNP}), and dehydrated collagen hydrogels (Dehyd H, Dehyd CH). (A) Hydrogel weight as a percent of pre-compression weight over 7 – 9 days of submersion in 1x PBS or Milli-Q water if the hydrogel contained AgNPs. H (n=3), CH (n=3), H^{AgNP} (n=2), CH^{AgNP} (n=4), Dehyd H (n=3), Dehyd CH (n=4). (B) Swelling weights of compressed hydrogels do not approach original pre-compression weights, even after full dehydration ($p<0.001$). Weight changes within a gel type were only significant in dehydrated hydrogels (not marked) and in CH gels ($p<0.01$) despite the change being small (21% increase).

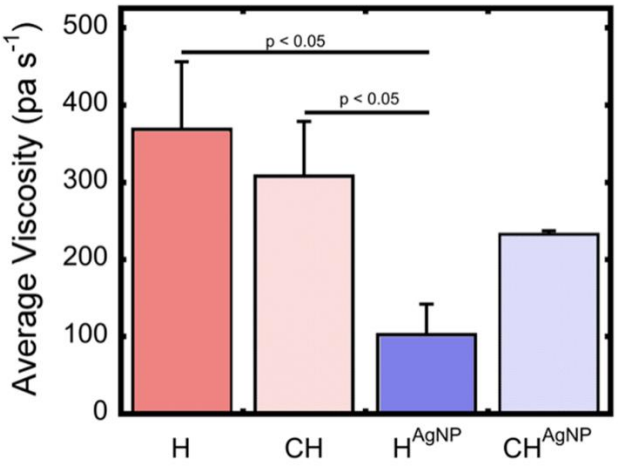

Figure 10. Average viscosity of unmodified collagen hydrogels (H), compressed collagen hydrogels (CH), and collagen hydrogels with AgNPs (H^{AgNP}, CH^{AgNP}). H^{AgNP} hydrogels were significantly less viscous than H ($p < 0.05$) and CH ($p < 0.05$) hydrogels. Significance is $p < 0.01$ when C and CH are grouped. Compression did not induce significant changes in viscosity for hydrogels without AgNPs ($p > 0.6$) and those with AgNPs ($p > 0.1$). Sample sizes were not large enough to show significance between CH^{AgNP} and H^{AgNP} despite the effect of compression roughly doubling the viscosity of H^{AgNP}. Sample sizes were: H (n=6), CH (n=7), H^{AgNP} (n=2), CH^{AgNP} (n=2).

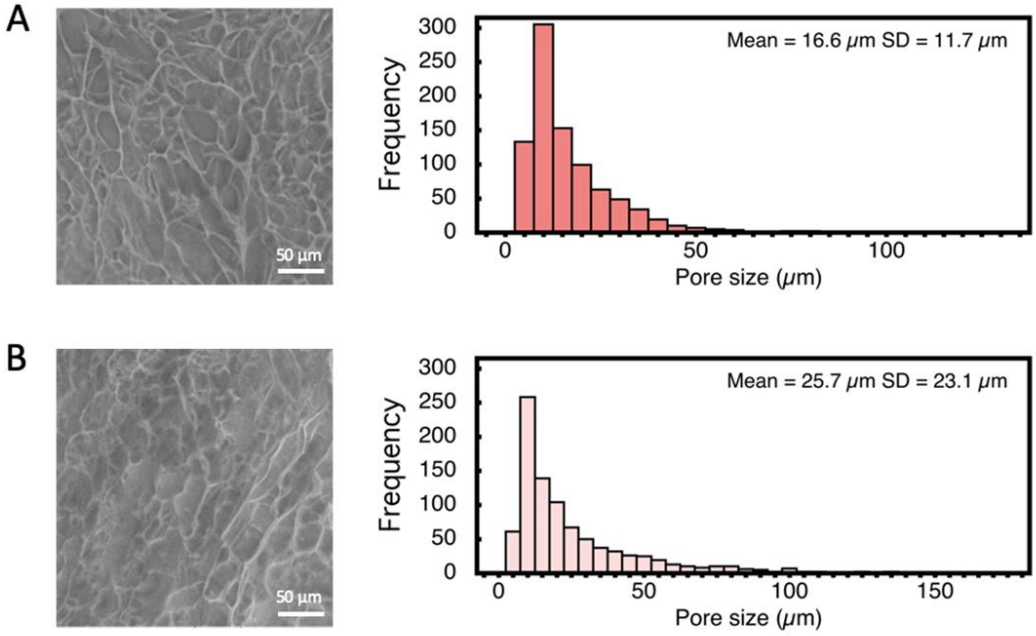

Figure 11. Frequency distribution of collagen pore sizes as a diameter (right) based on representative Cryo-SEM images (left). (A) Non-compressed hydrogel. (B) Compressed hydrogel. The mean pore diameter of compressed hydrogels is significantly greater than that of non-compressed hydrogels ($p < 0.001$) based on a student t-test.

6.4 Cell Viability on Compressed and AgNP Functionalized Hydrogels

A Live/Dead cell viability assay of human dermal fibroblasts seeded onto the various hydrogels revealed that AgNP functionalization resulted in a significant ≈96.5% to ≈6.99% drop in live cell percentages compared to hydrogels without AgNPs and a tissue culture plastic negative control ($p < 0.001$) (Figure 12). The total live cells counted on the AgNP functionalized gels were, in the best case, 105 times lower (from CH (n=6768) to CH^{AgNP} (n=67)), and in the worst case, up to 260 times lower (from H (n=8579) to H^{AgNP} (n=33)) than those found on the non-functionalized hydrogels. A proliferation assay was also performed (Figure 13), in which the proliferation of GFP transfected human dermal fibroblasts seeded into the various hydrogels was followed for 7 days.

Hydrogels functionalized with AgNP did not support cell proliferation over the 7 days while cells slowly proliferated on the non-functionalized hydrogels in comparison to the tissue culture plastic negative control. Additionally, apoptotic bodies during the proliferation assay can clearly be seen (Figure 14) on AgNP functionalized gels.

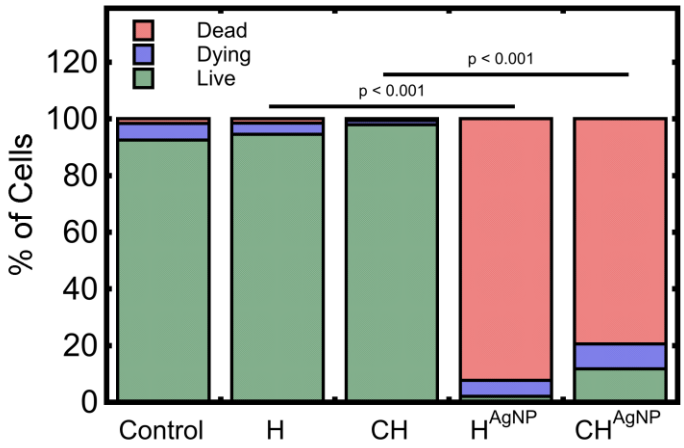

Figure 12. Cell viability assay on immortalized human fibroblasts grown on unmodified collagen hydrogels (H), compressed collagen hydrogels (CH), and collagen hydrogels with AgNPs (H^{AgNP}, CH^{AgNP}). The presence of AgNPs significantly reduced the % of Live cells compared to gels without AgNPs ($p < 0.001$). The CH group, compared to hydrogel free control, significantly increased the % of Live cells by 5.3% ($p < 0.001$; unmarked in figure), but was not significant in comparison to the H group ($p = 0.07$). The CH^{AgNP} had almost 10% more live cells than H^{AgNP} but was not significant due to the low cell counts in these groups. Lower total cell counts alone are an indicator for cytotoxicity. Total counted cell sample sizes including Live, Dying, and Dead cells: control (n=7857), H (n=9075), CH (n=6919), H^{AgNP} (n=1900), CH^{AgNP} (n=668).

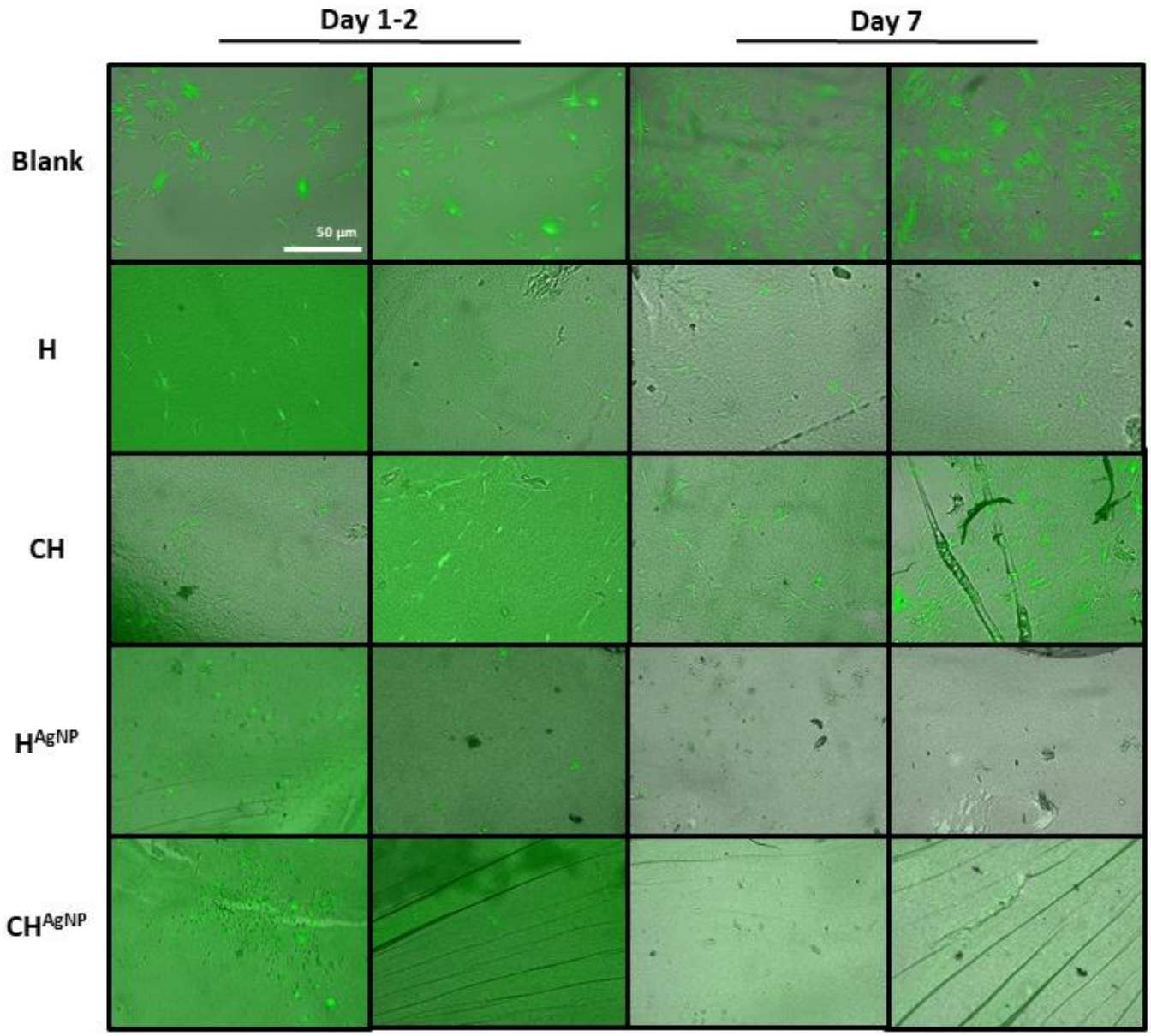

Figure 13. Multichannel (fluorescent/brightfield) images of a proliferation assay on collagen hydrogels (H), compressed collagen hydrogels (CH), and collagen hydrogels with AgNPs (H^{AgNP}, CH^{AgNP}) using green fluorescence protein (GFP) transfected immortalized human fibroblasts. (n=4 wells per group). While the control wells containing no hydrogel approached confluency at day 7, H and CH hydrogels did not support considerable proliferation while no proliferation was observed on AgNP functionalized hydrogels. Small, circular cell shapes observed on day 1with the AgNP functionalized hydrogels suggests there may have been no initial cell attachment or toxicity. 3 random images of each well were taken daily for 7 days.

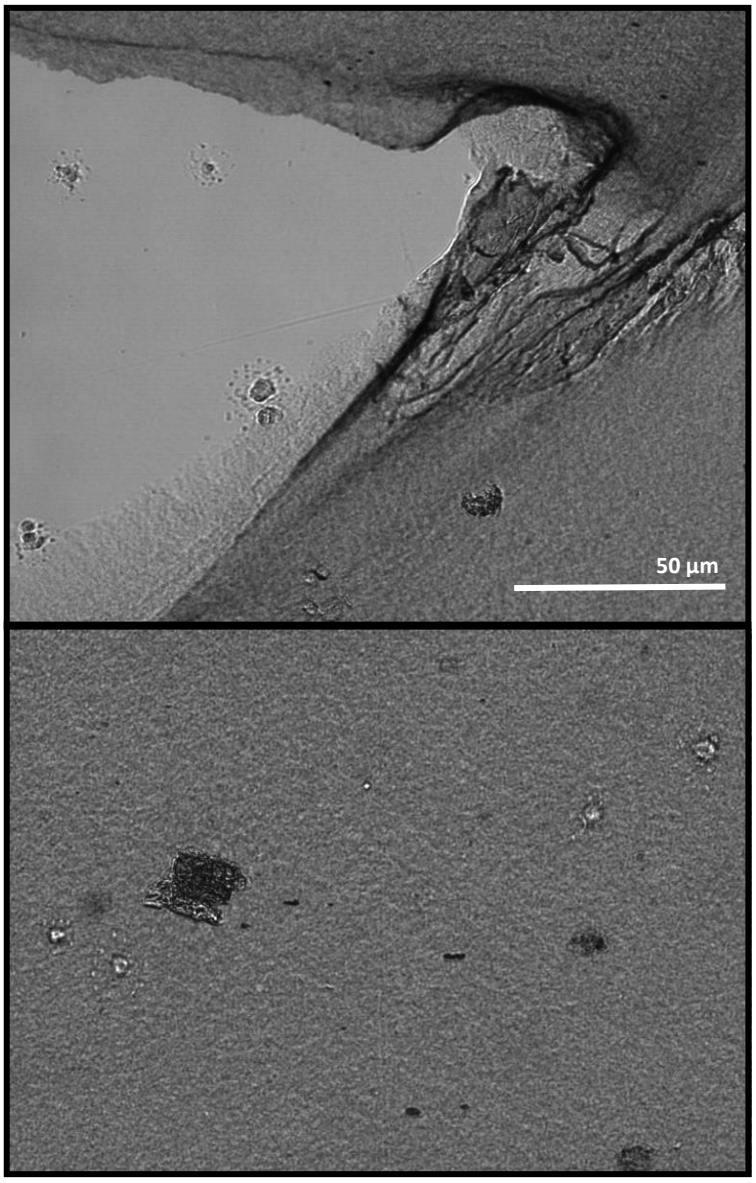

Figure 14. Brightfield (top) and darkfield (bottom) microscopic images of apoptotic human fibroblasts seeded on non-compressed (top) and compressed (bottom) AgNP functionalized collagen hydrogels taken 1 day after initial seeding.

7. Discussion

Collagenase Assay: How Compression and AgNP Functionalization Affected Collagen Hydrogel Degradability

For application of collagen hydrogels to be successful, they must take into consideration the dynamicity of the environment around an ulcer, particularly if the ulcer is infected. More often than not, infections may develop if proper preventative measures are not taken, such as proper cleaning of the site, wound off-loading, and in many cases the administration of prophylactic antibiotics. The complexity of microbiology in DFUs can determine the seriousness of the infection. For example, shorter duration DFUs typically have less microbial diversity containing mainly Gram-positive cocci, while chronic DFUs have highly complex microbial environments (Sadeghpour Heravi *et al.*, 2019). What is common among DFU colonizing bacteria is that they carry genes for pathogenicity factors such as collagenase proteases that digest the collagen in extracellular matrices further complicating the healing and wound closure process.

Collagenases also mark one of the greater pitfalls of collagen hydrogels since they too are degraded in the presence of bacteria that express the protease. Therefore, a key test in assessing the robustness of collagen hydrogels is to measure their susceptibility to collagenases by incubating the hydrogels with collagenase at 37°C. Since *in vivo* collagenase degradation can take weeks, the assay is performed at a much higher concentration of collagenase. This accelerates the degradation process so it may be completed within 24 hours. The hydrogel's weight is sampled over time and a rough estimate on its degradability can be established. Four types of hydrogel were exposed to collagenase; regular collagen hydrogels (H), compressed collagen hydrogels (CH), and both types additionally functionalized with AgNPs (H^{AgNP} and CH^{AgNP}). Results are summarized in section 6.1 (Figure 6).

AgNP functionalization had a positive initial effect on degradation rates when compared to non-functionalized hydrogels. This may be the result of silver's ability to inhibit collagenase enzymatic activity in the nanocrystalline form (AgNP); although, to a lesser degree, silver can also be inhibitory in its free cationic form (Ag^+) (Jovanovic *et al.*, 2012). Without performing an AgNP stability test, it cannot entirely be deduced if inhibition was mostly from Ag^0 found within NPs, or from Ag^+ NP oxidation products. A brown colouration within the AgNP hydrogels could indicate particle agglomeration and oxidation, however no browning was observed at the time of the assay. Thus, inhibition is less likely to be the result of Ag^+, unless excess silver nitrate (NP precursor) remained after *in situ* synthesis and washing.

The degradation rate (half-life) was calculated for all experimental groups based on the weight remaining at 4 hours, and 24 hours in the case of CH^{AgNP}. The reason for this is that its weight increased substantially (1.7x) by the 4 hour mark instead of decreasing or remaining stable as anticipated. The half life of H^{AgNP} gels was around 4 times greater ($t_{1/2} \approx 7 – 9$ hours) than non-functionalized gels ($t_{1/2} \approx 2$ hours), however without sampling weights beyond 4, hours it is difficult to assign a half life which is greater than 4 hours since the loss rate may not be linear after a certain period of time. Furthermore, the weights sampled at 24 hours might have plateaued earlier and thus might introduce some error in these measurements. If these experiments were to be repeated again, they could be performed using a lower concentration of collagenase so that sampling can be performed at intervals over multiple days.

Hydrogels that were both, compressed and functionalized with AgNPs (CH^{AgNP}), showed a significantly reduced rate of degradation (≈ 33%). At 24 hours these were the only hydrogels that still contained over one third of their initial weight, suggesting that compression and functionalization with AgNPs may have a synergistic effect that protects hydrogels from

collagenase degradation. Yet, it is also surprising to see a 70% increase in weight by the fourth hour despite all groups being hydrated in Tris-HCl solution for 1 hour at 37°C prior to initial weighing. At this point, it is hard to establish any conclusions on initial CH^{AgNP} degradation rates because the initial increase in weight convolutes the rate of degradation measurements. One possibility for the observed increase may be the uncertainty in measuring such small gel fragments (0.01 g – 0.1 g) on a milligram scale ($\pm$0.005g) after attempting to remove all fluids around the hydrogel. For example, if a fragment weighs 0.026 g and 0.020g of fluid remain on and under the hydrogel, a new total weight of 0.046g would indicate a ≈77% increase. This may also partially explain why H^{AgNP} gels did not experience the same gain in mass as the CH^{AgNP} gels, because H^{AgNP} fragments generally weighed more, decreasing the impact of experimental error. Another difference between CH^{AgNP} and H^{AgNP} gels is the factor of compression. One may suspect that compressed gels (whose water was pushed out) would decompress and swell back to their original weight which is roughly double the compressed weight. However, this should not occur since prior swelling tests confirmed compression is plastic and not sponge-like (Figure 9). The surprising gain in mass may instead be partially be explained by the osmotic activity of a silver, especially if NPs began to oxidize and Ag^+ began to draw water into the hydrogels. As such, CH^{AgNP} gel degradation rates during the first 4 hours are convoluted and likely do not provide conclusive information regarding the initial rate of loss. However, with that being said, functionalization with AgNPs combined with compression did have a positive effect on the average degradation rate measured over a 24 hour period.

Compression without AgNP functionalization had no measurable effect on degradability. This includes degradation during the initial 4 hours and over a 24 hour period. Based on other physical characterizations of CH hydrogels, the reason compression had no effect may be

attributed to the method of compression which did not profoundly modify physical properties. For example, viscosity was unaffected before and after compression suggesting physical robustness may not have been improved. Considering that gels were compressed to a point close to their mechanical tearing limit, increasing the pressure of compression would be unlikely to provide improvements. Thus, other possible methods for compression should be assessed in future experiments. A hypothetical and undocumented method could be dehydrating compression. The effect of dehydrating compression can be seen in Figure 9, where dehydrated gels only swelled to approximately 60% of their initial weight. Based on this observation, removal of water from the hydrogel may force collagen fibers to stack tightly together. This method can create ultrathin and perhaps stronger hydrogels once rehydrated. While thickness could be increased by stacking multiple layers, this could be a very impractical process given that dozens of hydrogels may need to be prepared to generate a single compressed hydrogel. Another alternative could be centrifugal compression, which would create a gradient of compression so that the deeper parts of the are denser without losing significant hydrogel thickness.

In conclusion, the assay should be attempted again at lower collagenase concentrations to verify the resistance of CH^{AgNP} gels towards collagenase degradation. Furthermore, AgNP stability should be assessed and sampled throughout a parallel assay to determine to what degree AgNPs are oxidized, and the rehydration process of all hydrogels should be extended from 1 hour to at least 4 hours in case hydrogels may have become partially dehydrated prior to experimentation. Lastly, compression alone did not yield any improvements in degradability, although this should not rule out compression as a method for improving hydrogel properties. Tests on hydrogel pore size and viscosity suggest that the method of compression may not have been impactful enough to

reap expected benefits of compression, such as those documented in literature (Pensalfini *et al.*, 2017). As such, other methods for compression should also be attempted.

Swelling and Solid Mass Content

As previously mentioned, maintaining a moist healing environment is essential for DFU wound closure. The developed hydrogels are approximately 96.72% water by weight, or 3.28% collagen by weight. Upon compression, roughly 50% of the hydrogel's weight in water is lost, thus doubling the SMC as illustrated in Figure 8. This confirms that compression has a significant initial impact on SMC. However, to ensure changes in physical characteristics were permanent, a swelling test was performed to measure potential decompression reflected by decreasing SMC over time.

Swelling tests inform us on how much water is reabsorbed after compression. The amount of water reabsorbed post-compression quantifies the hydrogel's ability to decompress. Similar to what happens when squeezing a kitchen sponge; water is expelled, decreasing water content, and increasing SMC. However, if submerged in water again, the sponge decompresses to its original volume and water mass. Thus, we can deduce that the physical properties of the sponge have not changed, and compression is not plastic. If a hydrogel remains compressed, it is said that compression is plastic.

Figure 9a illustrates how gel weights were stable throughout the swell. No upward trends were found suggesting decompression. Figure 9b highlights any significant changes in SMC observed from initial to final swelling weight. Despite CH gels showing a marginally significant change in weight from decompression, they remain at 40% of their original mass after 9 days of swelling. All comparisons between compressed and non compressed hydrogels were significant,

suggesting compression was plastic. Even after full dehydration and rehydration (Figure 9b, Dehydration columns), hydrogels maintain their water retention characteristics because compressed hydrogels rehydrated to only about half the value of non-compressed gels. This indicates that properties in microscopic collagen frameworks were maintained even after dehydration of the hydrogel. Therefore, this test confirmed that a permanent change in physical characteristics is induced by compression.

Rheology

Compression did not impart any significant changes in viscosity, although it appears that within AgNP functionalized hydrogels, compression led to increased viscosity. This result is not significant due to the limited sample sizes. It was surprising to see that compression did not affect viscosity considering SMC nearly doubled after compression (Figure 8) and a decrease in gel translucence occurred suggesting an increased collagen network density. Literature agrees that compression should improve mechanical properties of collagen hydrogels (Pensalfini *et al.*, 2017; Levis *et al.*, 2010; Brown *et al.*, 2005). Thus, our results are more likely suggest that the method of compression – used to prepare 5% collagen by weight hydrogels – was not impactful enough to impart mechanical improvements, than to suggest compression does not provide mechanical improvement.

Functionalization with AgNP significantly reduced gel viscosity in H^{AgNP} gels, but not in CH^{AgNP} gels despite an obvious trend in reduction. The lack of significance is limited by a sample size of only 2 effectively measured hydrogels. The small sample size may not be large enough to overcome the variability in hydrogel synthesis. Small batch to batch variations in pH during collagen cross-linking could affect the final collagen network density to a measurable degree.

Additionally, the reduction in viscosity may also be attributed to some UVA photo-degradation during the *in situ* functionalization process. It has been observed that collagen breaks down in the presence of UVC radiation showing markedly reduced triple helix content over time, but it is also a predictable effect knowing UVC radiation is absorbed by most materials (Jariashvili *et al.*, 2012). No reports of collagen's UVA photo-degradation have been found. As such, a simple experiment to assess hydrogel viscosity as a function of time exposed to UVA radiation can elucidate to what degree photo-degradation occurs. This quantification would be rather important when considering *in situ* AgNP functionalization methods.

Hydrogel Pore Size

Compression was predicted to induce a reduction in pore size (PS) by compressing collagen network density. Upon observation of compressed hydrogels, an obvious decrease in translucency was noted suggesting that density of collagen fibre networks increased, consequently decreasing the average PS. However, our computation of PS distribution yielded results suggesting the opposite: that compression of hydrogels increased average PS. Figure 11 shows two representative images of H and CH gels with pore diameter frequencies illustrated to their right. Despite appearing similar, CH gels had a greater average PS. Figure 16 in the appendix performs a Kolmogorov-Smirnov test on ($n > 800$) pores to show that cumulative PS distributions are different not due to chance ($p < 0.0005$) shifting to greater values from H to CH gels. There are two reasons that can explain the outcome. Firstly, compression of hydrogels may have damaged collagen networks on the surface instead of compacting them together. Microtears in networks would open larger pores than before as collagen is pushed apart, potentially skewing the mean. A cause for microscopic tearing can be a rough compression surface on the underside of the compression

device (Figure 1). Secondly, the method of automatic PS computation may have bias in terms of pore selection criteria. If image contrast is not high enough, then pores may be merged into one larger pore leading to an overestimated PS. This effect is defined as grouping bias (Appendix Figure 15). If average PS decreased, then the contrast between smaller pores would also decrease, ultimately increasing the likelihood for grouping bias, leading to overestimated PS values. The processing technique and its vulnerability is captured in Figure 15 of the appendix.

Collagen Hydrogel Toxicity after In Situ Functionalization with AgNPs

AgNP absorption generally ranges in the 400 – 500 nm range. Therefore, hydrogels containing AgNPs will exhibit an absorption peak in this range. Initially, the method used for functionalizing hydrogels by soaking them in colloidal AgNP (method 4. of Figure 3) was unsuccessful and hydrogels did not take up any of the particles. This was obvious since basic washes removed any evidence of AgNPs from their surface. Instead, an *in situ* method was used to grow the particles within the hydrogel and revealed a clear and unwashable colour change to yellow/red after photochemical synthesis of AgNPs. The *in situ* method was validated by monitoring the absorption spectrum of the hydrogels before and after functionalization and washing (Figure 7). The resulting absorption peak is further overlaid on the absorbance of citrate-capped AgNPs and is remarkably similar.

Based on prior characterizations of wavelength maxima for various sized AgNPs, a 420nm peak indicates an average particle size of 50nm (Paramelle, 2014). Particle size is an important consideration in establishing safety since prior work has suggested AgNPs less than 20nm in diameter can be cytotoxic to human cell lines (Liu *et al.*, 2010; Hernández-Sierra *et al.*, 2011). Thus, the measured absorbance peak at 420nm suggests particles are of a safe size. The

biocompatibility of collagen protected AgNPs has also previously been confirmed (Alarcon *et al.*, 2015). Unfortunately, the cell viability assays performed suggested that the particles or functionalization process results in a relatively toxic materials. This may be due to the introduction of toxic by-products or a high polydispersity of AgNPs. Even though the upper 10% of peak absorbance spans a range of 390nm to 475nm, suggesting a polydispersed NP population ranging10nm to 90nm in diameter, light scattering from the gel can exaggerate the actual width of the absorbance peak. Brown colouration in the hydrogel would also suggest larger particles. Thus, the hydrogel may not actually contain particles below 20nm. Either way, polydispersity is a function of many variables so controlling particle growth conditions is essential, especially if they are produced within a semi-solid hydrogel medium. For example, one should ensure that reaction rates for particle seeding and growth are consistent by evenly dispersing UVA radiation throughout the hydrogel.

The synthesized particles require further basic characterization to assess their nature. This includes X-ray photoelectron spectroscopy to analyze their state of oxidation, Scanning or Transition Electron Microscopy to better evaluate polydispersity and NP size, as well as electrophoretic mobility (EM) to assess NP surface charge (Zeta potential) to provide further information on stability and toxicity. Although, performing EM would be difficult on NPs supported within a semi-solid matrix. A higher degree of characterization should be performed after every instance of hydrogen functionalization to ensure the functionalized AgNP are of previously observed non-toxic nature (>20nm in diameter, not excessively dispersed in size, properly supported with collagen or capping agents, and not oxidized) before attempting comprehensive biocompatibility tests.

Tests for cell viability on functionalized hydrogels reveal that they were highly cytotoxic via a Live/Dead assay. Collagen hydrogels without AgNP showed similar cell viability to negative controls, while compressed collagen hydrogels showed an improvement. Compression of functionalized hydrogels also showed some improvements in cell viability but may not have been significant due to dwindling cell counts by the fifth day. The assay showed that compression, including both non-functionalized (CH) and functionalized (CH^{AgNP}) gels, may provide a more suitable environment for fibroblast survival compared to H and H^{AgNP} gels.

The conducted proliferation assay revealed that fibroblasts survived on H and CH materials but proliferated to a smaller degree relative to the plastic control. Furthermore, no proliferation was seen on H^{AgNP} and CH^{AgNP} gels. Despite the control group seeming to approach confluency, fibroblast density and population of H and CH gels on day 7 of proliferation were substantially lower than observed cell density on the day 5 of the Live/Dead assay. This inconsistency may suggest that an over-confluent cell population was lifted and applied during seeding, resulting in lower than expected proliferation rates during the assay. As such the results may not necessarily reflect the true supportive potential hydrogels offer towards fibroblast proliferation.

The assay also serves as a second line of evidence to highlight the cytotoxicity of AgNP functionalized hydrogels. Fibroblasts exposed to AgNP did not adhere to hydrogels (evidenced by their circular shape) and underwent apoptosis within a few days (Figure 14). There are multiple reasons for what may have induced cytotoxicity, although apoptosis is a first indicator for irreparable DNA damage. The exact mechanism for AgNP or Ag^{+} toxicity in human cells is unknown, but it may be the result of mitochondrial respiratory chain disruption or the production of reactive oxygen species that cause DNA damage leading to apoptosis (Asharani *et al.*, 2009).

Cytotoxicity can arise for four general reasons: excessive AgNP concentrations, size-dependent cytotoxic AgNPs, leftover silver nitrate precursor post *in situ* synthesis, and the presence of oxidized AgNPs due to particle instability. The first reason for cytotoxicity may have been excessively high AgNP concentrations, which cannot easily be estimated within semi-solid materials without fully digesting the material to resuspend AgNPs. Based on a relatively low absorbance at 420nm (around 0.22) and on prior AgNP concentration to absorbance values within AgNP collagen hydrogels (Alarcon *et al.*, 2015) the concentration was likely below 0.2 μM, which is not necessarily excessive for biocompatibility. This rules out the first reason.

The second reason entailing size-dependent AgNP toxicity was already discussed in terms of high AgNP polydispersity. The presence of AgNPs smaller than 20nm may have contributed to lower cell viability but is unlikely since browning suggested larger NPs and light scattering to widen absorbance spectra may overestimate true polydispersity.

A third and likely rationale is that leftover silver nitrate after *in situ* functionalization contributed to cytotoxicity. The preparation method involved soaking AgNP precursors, silver nitrate, into the hydrogel for an extended period of time prior to photochemical synthesis (irradiation). If not all precursor (Ag^+) was consumed then hydrogels may have continued to leach cytotoxic Ag^+ even after washing.

The fourth reason is particle oxidation and aggregation. Although this was not measured, a colour change from red to brown was observed between AgNP functionalization and the beginning of viability assays. Such colour change reflects increased particle agglomeration and oxidation that may have also leached Ag^+, which is otherwise cytotoxic (Greulich *et al.*, 2012). Even though UV stimulus for particle growth is no longer present after functionalization, particles may continue to grow size until their eventual cohesive forces pull them together to cause

aggregation, the process being accelerated by AgNP oxidation (Gorham *et al.*, 2012). Under UV-vis, this would be seen as a shift in peak towards the 500nm range because larger particles absorb lower energy radiation. The peak would also decrease because increasing the number of large AgNPs would decrease the concentration of small AgNPs. Particle oxidation and aggregation is favoured enthalpically, so ensuring surface particle protection within the hydrogel is essential and may be achieved with a slightly higher citrate concentration during synthesis. This observation is still surprising since limited and porous space within a hydrogel structure acts as a nanoscopic pot for NP synthesis and separation that can ultimately prevent aggregation (Zhao *et al.*, 2015). In future experiments, AgNP characterization should precede cell viability tests and cell viability tests should be performed on freshly made hydrogels before any observable colour change occurs to indicate AgNP oxidation or agglomeration.

8. Conclusion

This study provides a basic level of understanding into all the necessary characterizations required for designing a viable collagen hydrogel which may provide improved mechanical properties and antiseptic effects when applied towards DFUs. The effects of compression and AgNP functionalization had appeared to significantly reduce the activity of collagenase enzymes, while AgNP functionalization alone moderately reduced collagenase activity. This improvement in degradability marks a first step towards use in infected DFUs, however requires further characterization to fully understand the mechanism of collagenase inhibition and AgNP stability. Regarding the physical properties of developed hydrogels, despite changes in solid mass content, measures of viscosity and pore size did not reflect anticipated changes based on previous literature. Instead of increased viscosity and smaller pore size, compressed hydrogels experienced no change in viscosity and increased pore size. Attempts to yield large pore sample sizes ($n > 800$ pores) using computerized image processing on photos of variable contrast may have confounded actual pore size results with measurement grouping bias (Figure 15). The observed effects of compression, or lack thereof, are likely attributed to a non-impactful method of compression. That is to say, other compressive methods that increase SMC to a point beyond 5% may more clearly show improvements in physical and mechanical properties. Generally, compression's effect on degradability, viscosity, SMC, cell viability (Live/Dead) seemed to have larger effects on AgNP functionalized gels than those without AgNP. This may be due to non-compressed hydrogels being more vulnerable to UVA photo-degeneration during the *in situ* functionalization process than compressed hydrogels. In terms of biological properties analyzed via Live/Dead assay and proliferation assay, compressed hydrogels supported somewhat higher fibroblast survival and proliferations rates compared to their non-compressed counterparts. The AgNPs functionalized

were of an estimated diameter of 50nm, but without further characterization for AgNP stability and residual silver nitrate concentrations after functionalization, the reason for cytotoxicity cannot be distinguished between the NPs or their Ag^{+} counterparts. In conclusion, modifications for the method of compression should be considered with multiple variations in AgNP functionalization techniques to build upon the developed hydrogels that showed substantially improved resistance to degradation. This thesis provides future projects a better understanding regarding what steps and methods to use when developing new hydrogel formulations that should ultimately show improved mechanical, biological, and antiseptic properties for promising application in DFUs.

9. References

Alarcon, E., Griffith, M., & Udekwu, K. (2015). *Silver nanoparticle applications : in the fabrication and design of medical and biosensing devices* . https://doi.org/10.1007/978-3-319-11262-6

Alarcon, E., Udekwu, K., Noel, C., Gagnon, L., Taylor, P., Vulesevic, B., … Griffith, M. (2015). Safety and efficacy of composite collagen silver nanoparticle hydrogels as tissue engineering scaffolds. *Nanoscale*, *7*(44), 18789–18798. https://doi.org/10.1039/c5nr03826j

Asharani, P., Low Kah Mun, G., Hande, M., Valiyaveettil, S., & AshaRani, P. (2009). Cytotoxicity and genotoxicity of silver nanoparticles in human cells. *ACS Nano*, *3*(2), 279–290. https://doi.org/10.1021/nn800596w

Brown, R., Wiseman, M., Chuo, C., Cheema, U., & Nazhat, S. (2005). Ultrarapid Engineering of Biomimetic Materials and Tissues: Fabrication of Nano- and Microstructures by Plastic Compression. *Advanced Functional Materials*, *15*(11), 1762–1770. https://doi.org/10.1002/adfm.200500042

Chai, Q., Jiao, Y., Yu, X., & Chai, Q. (2017). Hydrogels for Biomedical Applications: Their Characteristics and the Mechanisms behind Them. *Gels (Basel, Switzerland)*, *3*(1). https://doi.org/10.3390/gels3010006

Cushing, B.L., Kolesnichenko, V.L., O'Connor, C.J. (2004). Recent advances in the liquid-phase syntheses of inorganic nanoparticles. Chem. Rev. **104**, 3893–3946

Dumville, J., O'Meara, S., Deshpande, S., & Speak, K. (2013). Hydrogel dressings for healing diabetic foot ulcers. *Cochrane Wounds Group*, *2017*(7), CD009101. https://doi.org/10.1002/14651858.CD009101.pub3

Driver, V., Fabbi, M., Lavery, L., & Gibbons, G. (2010). The costs of diabetic foot: The economic case for the limb salvage team. *Journal of Vascular Surgery*, *52*(3), 17S–22S. https://doi.org/10.1016/j.jvs.2010.06.003

Everett, E., & Mathioudakis, N. (2018). [Review of Update on management of diabetic foot ulcers]. Annals of the New York Academy of Sciences, 1411(1), 153–165. https://doi.org/10.1111/nyas.13569

Galdiero S., Falanga A., Vitiello M., Cantisani M., Marra V., Galdiero M. Silver nanoparticles as potential antiviral agents. Molecules (Basel, Switzerland) 2011;16:8894–8918. doi: 10.3390/molecules16108894

Gorham, J., MacCuspie, R., Klein, K., Fairbrother, D., & Holbrook, R. (2012). UV-induced photochemical transformations of citrate-capped silver nanoparticle suspensions. *Journal of Nanoparticle Research*, *14*(10), 1–16. https://doi.org/10.1007/s11051-012-1139-3

Greulich, C., Braun, D., Peetsch, A., Diendorf, J., Siebers, B., Epple, M., & Kller, M. (2012). The toxic effect of silver ions and silver nanoparticles towards bacteria and human cells occurs in the same concentration range. *RSC Advances*, *2*(17), 6981–6987. https://doi.org/10.1039/c2ra20684f

Hernández-Sierra, JF., Galicia-Cruz, O., Salinas-Acosta, A., Ruíz, F., Pierdant-Pérez, M., and Pozos-Guillén, A. (2011) In vitro Cytotoxicity of Silver Nanoparticles on Human Periodontal Fibroblasts. Journal of Clinical Pediatric Dentistry: September 2011, Vol. 36, No. 1, pp. 37-42. https://doi.org/10.17796/jcpd.36.1.d677647166398886

Hilton, J., Williams, D., & Miller, D. (2004). Wound Dressings in Diabetic Foot Disease. *Clinical Infectious Diseases*, *39*, S100–S103.

Holmes, C., Wrobel, J., Maceachern, M., Boles, B., & Holmes, C. (2013). Collagen-based wound dressings for the treatment of diabetes-related foot ulcers: a systematic review. *Diabetes, Metabolic Syndrome and Obesity : Targets and Therapy*, *6*, 17–29. https://doi.org/10.2147/DMSO.S36024

Hui-Li Tan, Sin-Yeang Teow, & Janarthanan Pushpamalar. (2019). Application of Metal Nanoparticle–Hydrogel Composites in Tissue Regeneration. *Bioengineering*, *6*(1). https://doi.org/10.3390/bioengineering6010017

Jariashvili, K., Madhan, B., Brodsky, B., Kuchava, A., Namicheishvili, L., & Metreveli, N. (2012). Uv damage of collagen: Insights from model collagen peptides. *Biopolymers*, *97*(3), 189–198. https://doi.org/10.1002/bip.21725

Jovanovic A., Ermis R., Mewaldt R., Shi L., Carson D. (2012). The Influence of Metal Salts, Surfactants, and Wound Care Products on Enzymatic Activity of Collagenase, the Wound Debriding Enzyme. *WOUNDS*. 2012;24(9):242–253.

Levis, H., Brown, R., & Daniels, J. (2010). Plastic compressed collagen as a biomimetic substrate for human limbal epithelial cell culture. *Biomaterials*, *31*(30), 7726–7737. https://doi.org/10.1016/j.biomaterials.2010.07.012

Li, S., Dong, S., Xu, W., Tu, S., Yan, L., Zhao, C., … Chen, X. (2018). [Review of *Antibacterial Hydrogels*]. *Advanced Science*, *5*(5), n/a–n/a. https://doi.org/10.1002/advs.201700527

Liu, W, Wu, Y, Wang, C. Impact of silver nanoparticles on human cells: effect of particle size. Nanotoxicology 2010; 4: 319–330.

nanoComposix©. (2020). Salt Stability of Nanoparticles. Retrieved March 14, 2020 from https://nanocomposix.com/pages/salt-stability-of-nanoparticles.

Poblete, H., Manuel Ahumada, M., Jacques, E., Andronic, C., Comer, J., & Alarcon, E. (2018). CLK-Peptides as Superior Surface Stabilizers for Silver Nano Structures: Role of Peptide Chain Length and Applications in Nanomedicine. *Biophysical Journal*, *114*(3), 543a–543a. https://doi.org/10.1016/j.bpj.2017.11.2966

Paramelle, D., Sadovoy, A., Gorelik, S., Free, P., Hobley, J., & Fernig, D. (2014). A rapid method to estimate the concentration of citrate capped silver nanoparticles from UV-visible light spectra. *The Analyst*, *139*(19), 4855–4861. https://doi.org/10.1039/c4an00978a

Pensalfini, M., Ehret, A., Stüdeli, S., Marino, D., Kaech, A., Reichmann, E., & Mazza, E. (2017). Factors affecting the mechanical behavior of collagen hydrogels for skin tissue engineering. *Journal of the Mechanical Behavior of Biomedical Materials*, *69*, 85–97. https://doi.org/10.1016/j.jmbbm.2016.12.004

Sadeghpour Heravi, F., Zakrzewski, M., Vickery, K., G Armstrong, D., Hu, H., & Sadeghpour Heravi, F. (2019). Bacterial Diversity of Diabetic Foot Ulcers: Current Status and Future Prospectives. *Journal of Clinical Medicine*, *8*(11). https://doi.org/10.3390/jcm8111935

Singh P., Ahn S., Kang J.P., Veronika S., Huo Y., Singh H., Chokkaligam M., El-Agamy Farh M., Aceituno V.C., Kim Y.J., et al. In vitro anti-inflammatory activity of spherical silver nanoparticles and monodisperse hexagonal gold nanoparticles by fruit extract of Prunus serrulata: A green synthetic approach. Artif. Cells Nanomed. Biotechnol. 2018;46:2022–2032. doi: 10.1080/21691401.2017.1408117.

Slavin, Y., Asnis, J., Hafeli, U., & Bach, H. (2017). Metal nanoparticles: understanding the mechanisms behind antibacterial activity. *Journal Of Nanobiotechnology*, *15*(1), 65. https://doi.org/10.1186/s12951-017-0308-z

Teow S.Y., Wong M.M., Yap H.Y., Peh S.C., Shameli K. Bactericidal Properties of Plants-Derived Metal and Metal Oxide Nanoparticles (NPs) Molecules (Basel, Switzerland) 2018;23:1366. doi: 10.3390/molecules23061366

Wang, M., Marepally, S., Vemula, P., & Xu, C. (2016). Chapter 5 - Inorganic Nanoparticles for Transdermal Drug Delivery and Topical Application. In *Nanoscience in Dermatology* (pp. 57–72). https://doi.org/10.1016/B978-0-12-802926-8.00005-7

Waterman-Storer, C., & Waterman-Storer, C. (2001). Microtubule/organelle motility assays. Current Protocols in Cell Biology, chapter 13(1), Unit 13.1–Unit 13.1. https://doi.org/10.1002/0471143030.cb1301s00

Zhao F., Yao D., Guo R., Deng L., Dong A., Zhang J. Composites of Polymer Hydrogels and Nanoparticulate Systems for Biomedical and Pharmaceutical Applications. Nanomaterials (Basel, Switzerland) 2015;5:2054–2130. doi: 10.3390/nano5042054.

Zhang P., Lu J., Jing Y., Tang S., Zhu D., Bi Y. Global epidemiology of diabetic foot ulceration: A systematic review and meta-analysis (dagger) Ann. Med. 2017;49:106–116. doi: 10.1080/07853890.2016.1231932.

10. Appendix

Stepwise rearrangement of the half life equation:

$$N_t = N_0\ 0.5^{\frac{t}{t_{\frac{1}{2}}}}$$

$$(\%wt_t) = (100\%)\ 0.5^{\frac{t}{t_{\frac{1}{2}}}}$$

$$log_{\frac{1}{2}}(\frac{\%wt_t}{100\%}) = log_{\frac{1}{2}}(0.5^{\frac{t}{t_{\frac{1}{2}}}})$$

$$log_{\frac{1}{2}}(\frac{\%wt_t}{100\%}) = \frac{t}{t_{\frac{1}{2}}}$$

$$t_{\frac{1}{2}} = \frac{t}{log_{\frac{1}{2}}\left(\frac{\%wt_t}{100\%}\right)}$$

$$t_{\frac{1}{2}} = \frac{t \times (-ln2)}{ln\left(\frac{\%wt_t}{100\%}\right)}$$

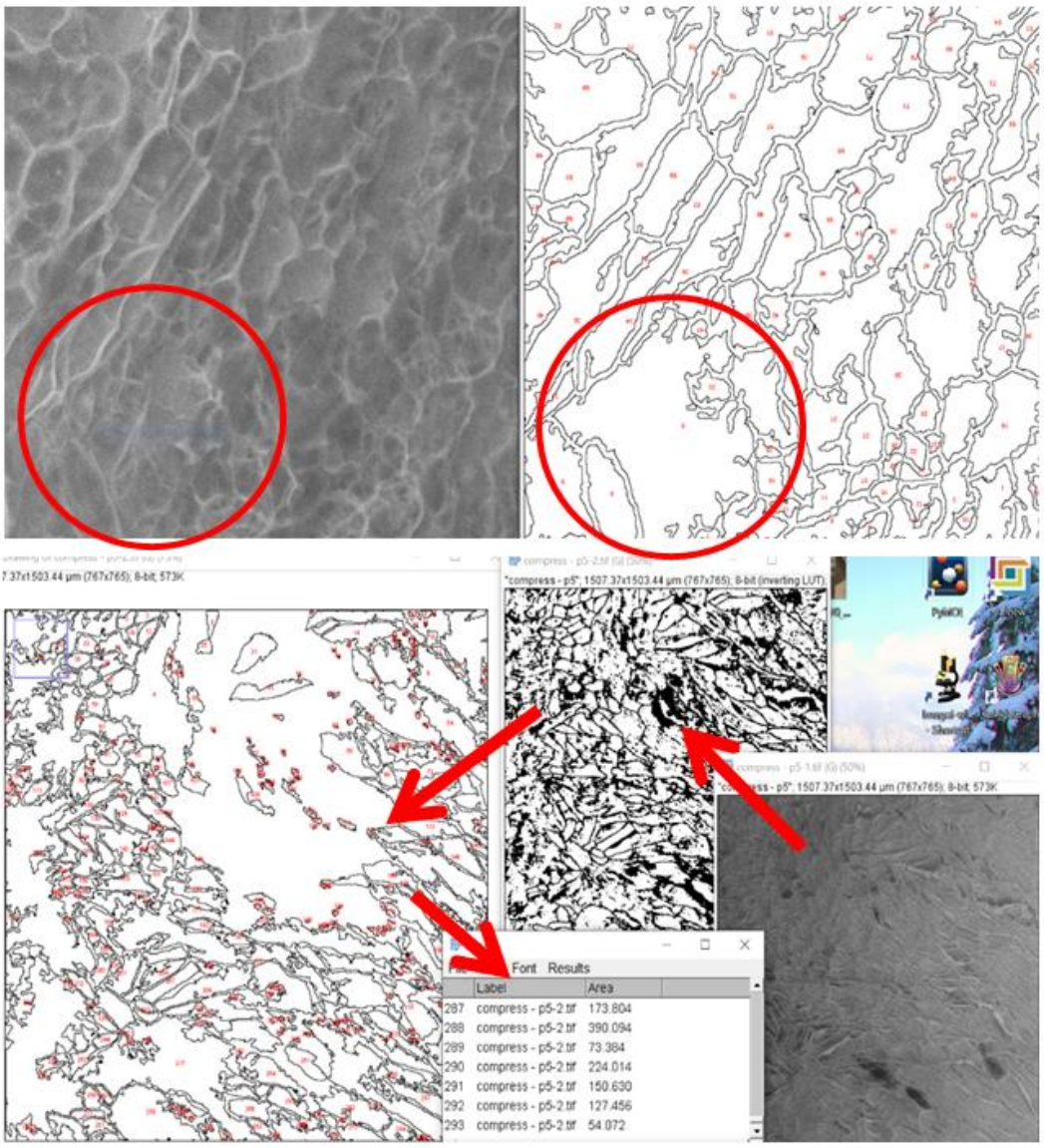

Figure 15. Illustration of computerized pore size processing of Cryo-SEM imaging. The upper half of the figure illustrates how grouping bias (red circle) can lead to pore size overestimation by grouping multiple smaller pores into one larger pore due to imperfect colour binarization. The bottom half illustrates the processing steps, where the image is initially binarized (black / white), then processed via the *analyze particles* function which counts and measures all pores that are fully enclosed, while combining pores that are connected (even by a single pixel) confounding true pore size distributions.

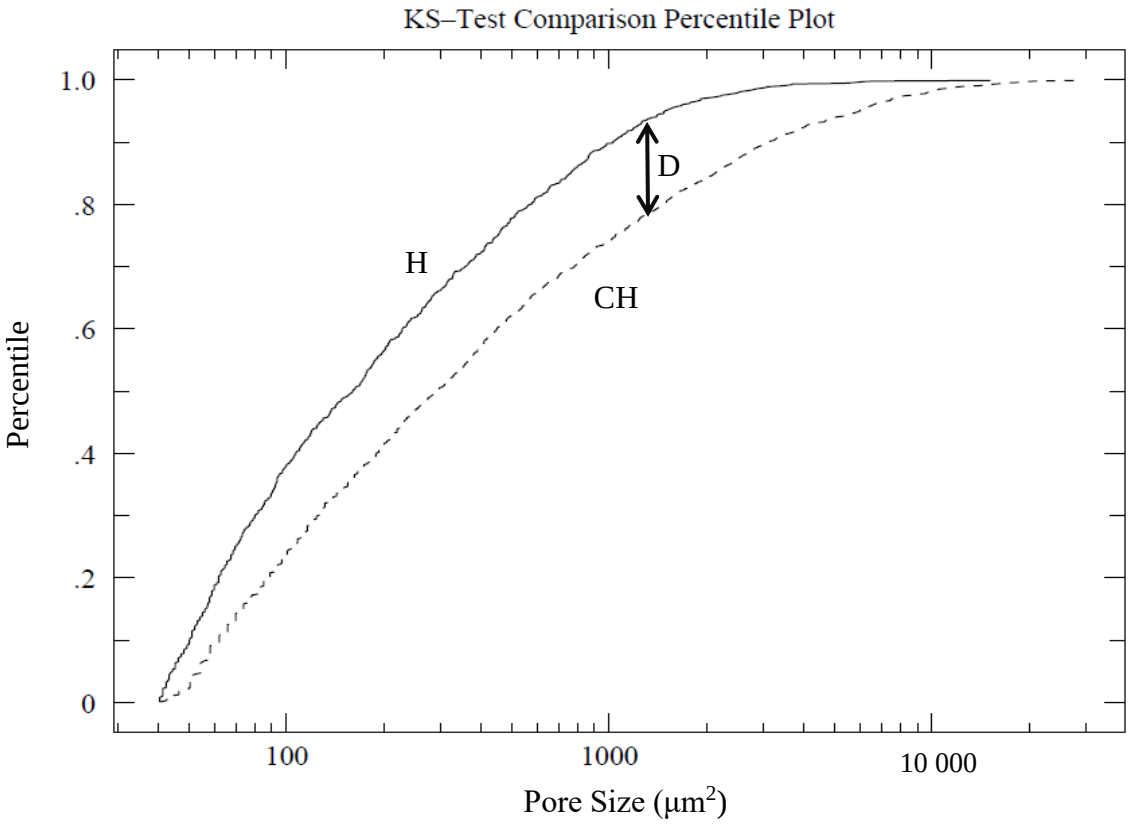

Figure 16. Kolmogorov-Smirnov cumulative distribution collagen pore size (μm^2) of non-compressed and compressed hydrogel pore sizes. The maximum difference between the cumulative distributions, D, is: 0.1653 with a corresponding $P < 0.0005$. Non-compressed hydrogel pores (n=886) and compressed hydrogel pores (n=902) were measured based on Cryo-SEM imaging as described in 5.9. Plot was developed using http://www.physics.csbsju.edu/ data entry window for KS testing.